# NOAA/NGDC candidates for IGRF-11

- Version 3 -

S. Maus and C. Manoj (NOAA/NGDC and CIRES, University of Colorado)
J. Rauberg, I. Michaelis and H. Lühr (Deutsches GeoForschungsZentrum, GFZ)

This submission includes candidates for all three products, namely the main field in 2005, the predicted main field in 2010, and the predicted secular variation 2010-2015.

## *Data Selection*

Due to the well-known spatial aliasing and crustal bias problems with ground-based observatory data, only satellite data were used in the actual model estimation. However, ground-based observatory data played an important role in data selection by providing the source of the Dst and $a_m$ indices.
The candidate models were entirely based on data from the CHAMP satellite. Ørsted data were processed simultaneously and used for validation of the processing steps and parent models. Ørsted data were also used in estimating the uncertainties of the Gauss coefficients.
All satellite data were sub-sampled to 20 seconds, corresponding to about 150 km along-track spacing. Separate data sets were compiled for mid latitudes (-60 to 60 magnetic latitude) and Polar Regions (> 50 and <-50 degrees). Vector data were only used at mid latitudes. Scalar and vector data at mid latitudes were selected for 22:00-5:00 local time for CHAMP and 20:00-5:00 LT for Ørsted. Data in the Polar Regions were used at all local times. No exclusion for solar zenith angle was made.

### General data selection criteria:

Maximum Dst: ± 30 nT
Maximum diamagnetic effect: 5.0 nT
Maximum jump in diamagnetic effect: 2.0 nT

### Polar regions specific criteria:

Max Dst derivative: 5nT/h
Max IMF-By: ± 8 nT
Min IMF-Bz: -2 nT
Max IMF-Bz: 6 nT
Max merging electric field at the magnetopause: 0.8 mV/m
Max $a_m$: 27
Max $a_m$ 3 hours before: 27

### Low latitude specific criteria:

Max Dst derivative: 2nT/h
Max $a_m$: 12
Max $a_m$ 3 hours before: 15

**CHAMP specific criteria:**

- Attitude from dual-head star camera mode
- Electron density and temperature measurements available

In a final data selection step, the RMS of along-track residuals against POMME-5 were sorted by longitude of the equator crossing and by date, separately for mid latitude, northern and southern tracks. Then the following test was carried out for each track: Its RMS value was compared with the RMS value of all neighboring tracks within 8 degrees distance in longitude and within one year difference in time. If it was found that this track had at least one neighbor to the east and another neighbor to the west with at least 3 nT smaller RMS, then this track was declared as "noisy" and was eliminated from the data set. Thus, the absolute residuals against POMME-5 were not a selection criterion. Instead, the relative agreement with POMME-5, as compared with neighboring tracks was used.

## *Corrections for instrument misalignment, plasma and ocean tidal effects*

The following corrections were applied to the data:

1. Estimated angular corrections for the misalignment between the magnetometer reference system and the star tracker reference system for the CHAMP satellite are used to correct the vector data accordingly.
2. The magnetic signals of motional induction in the oceans due to the 8 major tidal constituents up to spherical harmonic degree 45 are subtracted, as predicted by Kuvshinov and Olsen (2004).
3. The signature of plasma pressure driven currents is subtracted using the correction for the "diamagnetic effect", as proposed by Lühr et al. (GRL, 2003), making use of actual electron density and temperature measurements of CHAMP.

## *Corrections for magnetospheric fields*

Due to the local-time asymmetry of the magnetospheric fields, day-side data have to be included in their modeling. Since day-side data are too noisy for being included in the modeling of the main field, the magnetospheric fields are best estimated in a separate, preceding step. We used a revised version of the model described in Maus and Lühr (2005). This 18-parameter model quantifies the quiet-time magnetospheric fields, modulated by the Interplanetary Magnetic Field and solar activity. Details of the model will be described in a separate publication.

## *Parent model descriptions*

All parent models include:

1. The static part of the internal field to degree and order 40
2. The secular variation (SV) to degree and order 16
3. The secular acceleration (SA) to degree and order 16

4. A daily varying degree-1 external field, as proposed by Olsen et al. (2006) parameterized by a single value of the strength of an axial dipole in Solar-Magnetic, SM frame for every 24h interval.

The model coefficients were estimated in a non-iterative least-squares approach, where the information from the scalar data was linearized using POMME-5 as a starting model. The SV was regularized starting at degree and order 14, while the SA coefficients were damped for degrees 9 and higher.

Parent models were produced for two epochs:

1. To estimate the main field in 2005.0, we chose satellite data from 2003.5 to 2006.5. The primary parent model was produced from CHAMP data only. A second parent model was produced by including Ørsted scalar data. This model was only used for validation and to estimate the uncertainty of the coefficients of the first model
2. To predict the main field in 2010.0 and the secular variation 2010-2015, we used the last three years of available data, spanning 2006.5-2009.67. Again, the primary parent was based only on CHAMP data, while a second parent model including Ørsted data was used for estimating Gauss coefficient uncertainties

## *Derivation of candidate model coefficients and uncertainties*

The following procedures were use to derive the three candidate products and the uncertainties of the coefficients:

1. The main field in 2005.0 was simply taken as the static coefficients at the center of the CHAMP-only model. Their uncertainty was estimated by taking the difference to the corresponding coefficients of the model including Ørsted data, and multiplying the difference by three. The ad-hoc rationale for the factor three was that the Ørsted data had 1/3 weight in the combined model, so a “pure” Ørsted model would presumably exhibit three times the observed deviation to the CHAMP-only model. A minimum uncertainty of 0.01 nT was imposed in order to reflect the added uncertainty due to rounding errors.
2. The main field in 2010.0 was predicted by evaluating the Taylor series using secular variation and secular acceleration coefficients for the date 2010.0. The uncertainties were evaluated in the same way as for the 2005 model.
3. Studies of for- and hind-cast of the secular variation of the geomagnetic field (e.g. Maus et al, 2008) suggest that the predictive quality of the secular acceleration may be very limited. Taking a pessimistic view, we therefore provide the SV of the parent model at the end of the data interval (2009.67) as our best estimate of the SV 2010-2015. The primary uncertainty in SV forecast lies in the unpredictable behavior of the SA. As an estimate of uncertainty combining measurement and prediction uncertainties, we therefore take the difference between the SV of the CHAMP-model in 2009.67 and the forward-extrapolated SV of the combined model to 2012.5.

## *Test models with extended-degree secular variation*

We provide two models with extended-degree secular variation prediction. Both models are based on the SV at the end of the data interval (2009.67):

1. The extended-degree model corresponding to our candidate model submission for SV-2010-2015 based only on CHAMP data
2. The extended-degree model estimated from a combination of CHAMP and Ørsted data, which was used for the uncertainty estimation of products (2) and (3).

## *Parent model residual maps and tables*

The parent models were first validated against the CHAMP data from which they were produced. Subsequently, they were validated against Ørsted scalar data. The latter constitutes a truly independent validation since Ørsted data was neither used in the production of these models, nor in the production of POMME-5 which played a role as a reference model in the data selection and in the linearization of the inverse problem. All residuals are calculated as measurement minus model value.

Table 1: Residuals of satellite data against the two CHAMP-only parent models. There is a slight reduction in RMS in all vector components from the earlier to the later period due to the declining solar cycle. The Ørsted scalar data indicate a systematic bias of about 1.5 nT against both models.

| Data type | $X_m$(nT) | $X_{RMS}$(nT) | $Y_m$(nT) | $Y_{RMS}$(nT) | $Z_m$(nT) | $Z_{RMS}$(nT) | $F_m$(nT) | $F_{RMS}$(nT) |
|---|---|---|---|---|---|---|---|---|
| Parent model 2005, data range 2003.5 to 2006.5 | | | | | | | | |
| CHAMP vector (mid-lat.) | 0.2 | 3.3 | 0.2 | 3.8 | -0.1 | 2.7 | 0.1 | 2.5 |
| CHAMP scalar (global) | | | | | | | -0.2 | 3.2 |
| Ørsted scalar (global) | | | | | | | 1.1 | 2.6 |
| Parent model 2010, data range 2006.5 to 2009.67 | | | | | | | | |
| CHAMP vector (mid-lat.) | 0.3 | 3.1 | 0.1 | 3.0 | -0.4 | 2.2 | 0.1 | 2.4 |
| CHAMP scalar (global) | | | | | | | -0.1 | 3.1 |
| Ørsted scalar (global) | | | | | | | 1.4 | 2.4 |

CHAMP vector component residuals against the two CHAMP-only parent models are displayed in Figure 1. The Scalar residuals for CHAMP and independent Ørsted data are shown in Figure 2. The Ørsted residuals show a consistent positive offset of about 1 nT, meaning that Ørsted measures a stronger field than the models predict for that altitude. This is consistent with the mean values in Table 1.

To investigate whether the difference between CHAMP and Ørsted residuals is due to a genuine difference in the field strength, the mean residual against POMME-6 is plotted in Figure 3 as a time series. A genuine effect should be persistent and could be solar cycle dependent. Instead, the CHAMP and Ørsted residuals are in good agreement until 2003 and then subsequently deviate by about 1.5 nT, indicating a possible baseline shift of one of the scalar magnetometers. While the Ørsted residuals show a prominent 800-day periodicity coupled to its local time variation, a corresponding 110-day cycle is not visible in the CHAMP data.

Plotting the mean residual after 2005.0 against latitude in Figure 4 reveals that the difference between Ørsted and CHAMP is almost negligible at the equator, and peaks at about 40° latitude. However, whether the shift is due to Ørsted or CHAMP is difficult to deduce with certainty from the data alone.

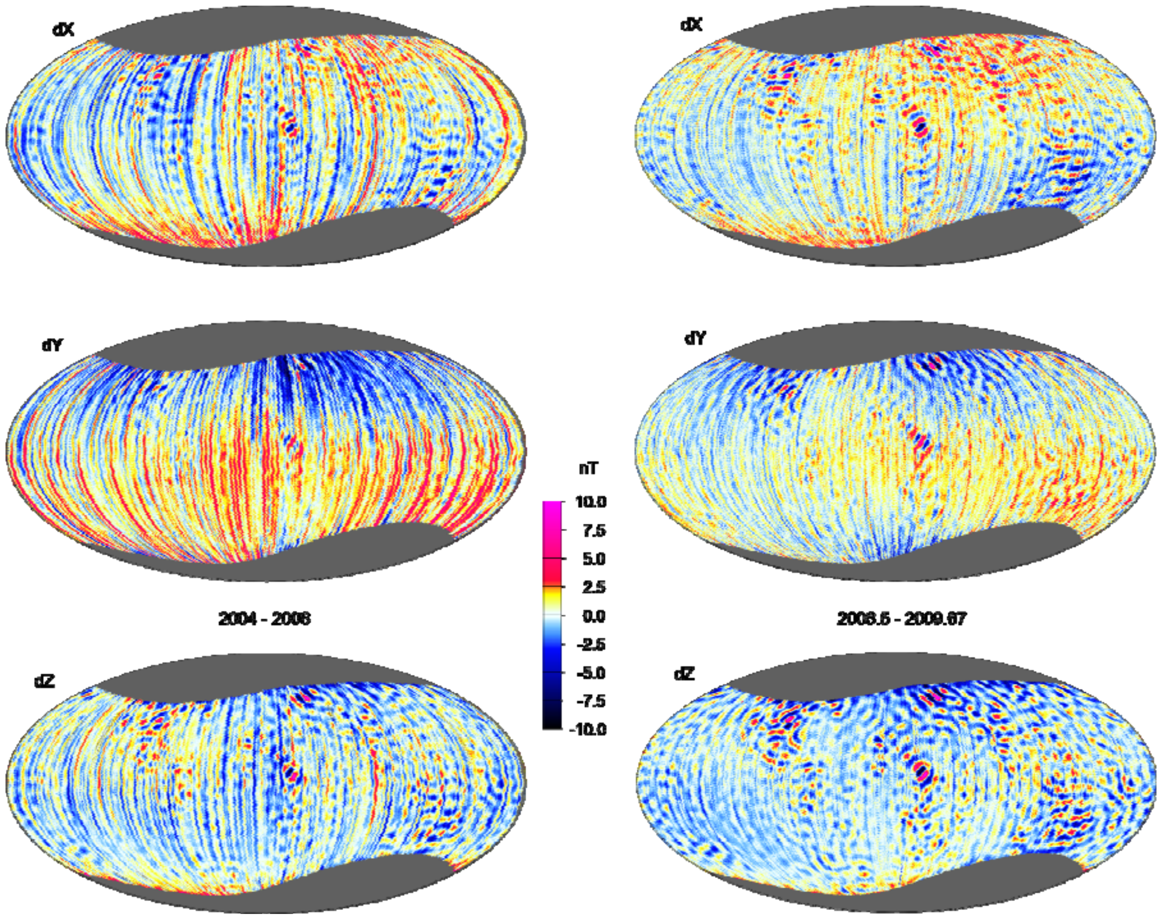


Fig 1: Vector component residuals of the two CHAMP-only parent models against the data that were used to estimate the model coefficients. The small-scale “bubbly” features are due to unmodeled crustal field beyond the model cut-off at degree 40. These features are stronger in the column on the right side due to the lower altitude of the CHAMP satellite. Furthermore, one can see that the residuals are significantly more noisy (striped patterns) in the earlier years, represented in the left column. This solar activity dependent difference is clearly visible despite the rigorous data selection criteria employed.

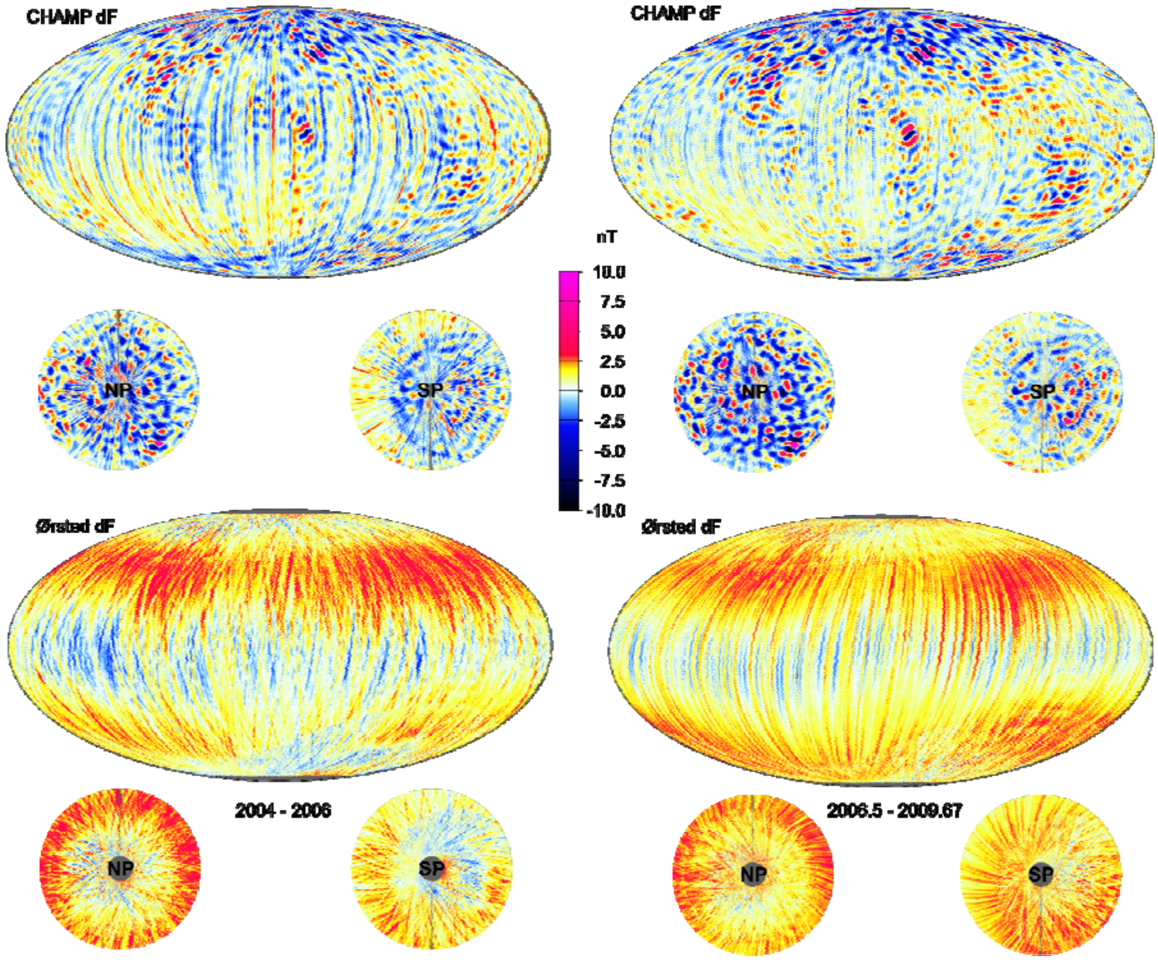


Fig. 2: Scalar residuals of the two CHAMP-only parent models against CHAMP scalar data (top row) and independent Ørsted scalar data (bottom row).

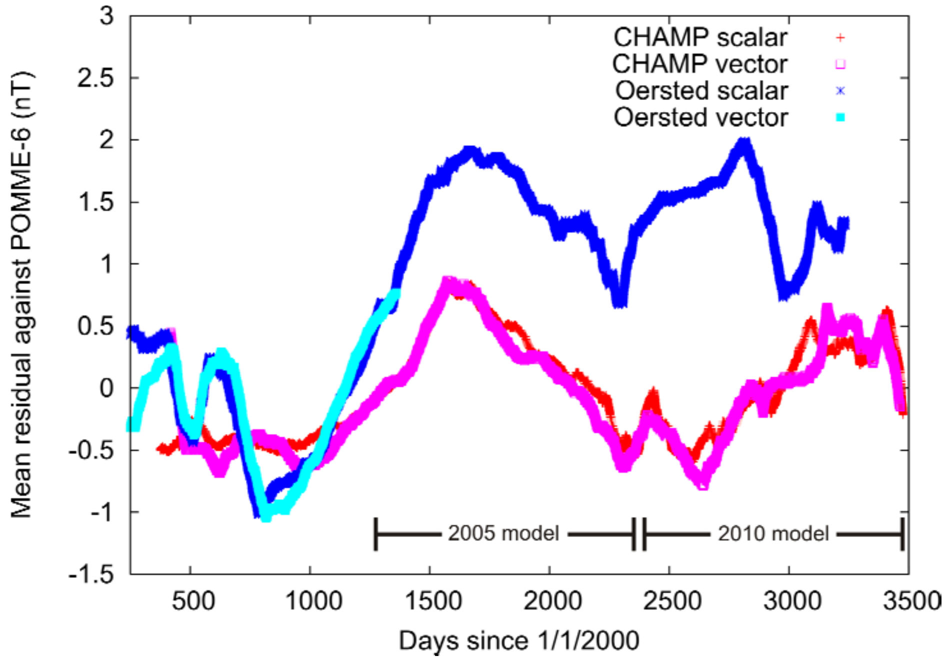


Fig.3: Evolution of the mean residual against POMME-6 over time. After 2004.0 (day 1460) we find a significant offset between the residuals of the two satellites. In addition, the Ørsted residuals exhibit a 800-day local time variation.

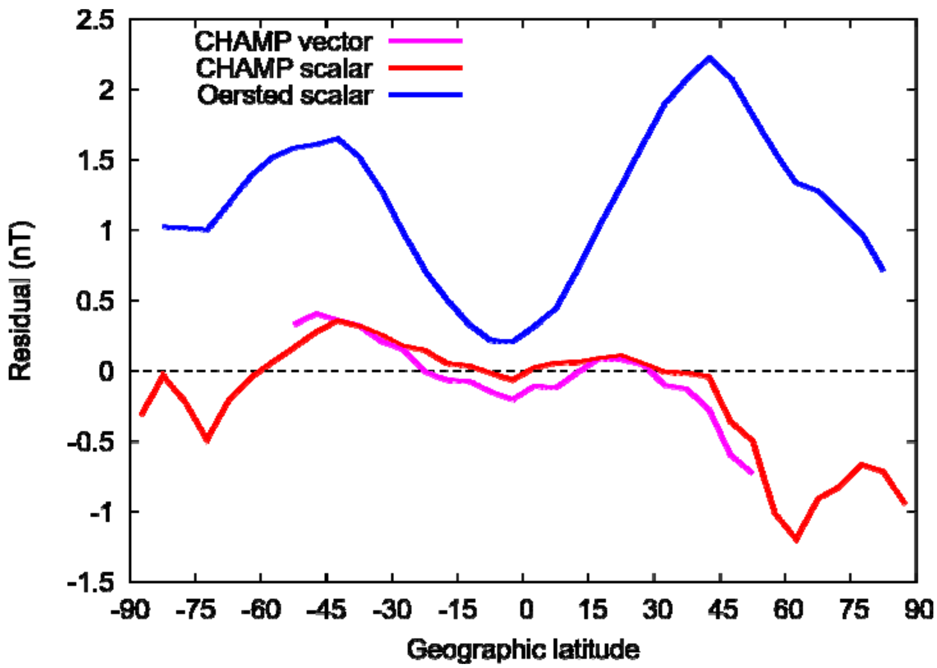


Fig. 4: Mean data residual against POMME-6 with geographic latitude, averaged over all longitudes in the time interval 2005.0 to 2009.67. There is only a marginal difference between plotting the residuals against geographic or magnetic latitude.

## *Summary*

Candidates for IGRF-11 have been derived from CHAMP satellite data and validated with Ørsted satellite data. Judging from the small residuals of the data against the models, an overall accuracy of the order of a few nT per component (at least at mid latitudes) has likely been achieved for the main field candidate for 2005. For the prediction of the main field at epoch 2010 somewhat larger and for the SV 2010-2015 much larger inaccuracies must be assumed, due to inherent problems with forecasting the future evolution of the geomagnetic field. An important question is whether the presently observed secular acceleration can be used to extrapolate the SV to the center of the upcoming epoch. Our analysis of past field behavior indicates that this is highly speculative. We have therefore taken the conservative approach of using the modeled SV at the end of the data period as an estimate of the SV for the upcoming epoch.

As an interesting secondary result, we find a systematic difference between the field strengths predicted by the CHAMP model and the Ørsted measurements at a different altitude. The Ørsted residuals exhibit an additional 800 day local time periodicity. These scalar residuals show a systematic latitude variation. Peak values occur just at latitudes (~40°) where the magnetic field of the ring current does not contribute to the field magnitude. However, the discrepancy does not exhibit a behavior over time that confirms a genuine difference in the ambient field strength. We are therefore not sure whether the differences are due to a deficit in external field separation or a deviation between the scalar magnetic field readings of the two spacecraft.

## *References*


Kuvshinov, A., and N. Olsen (2004), 3-D modelling of the magnetic fields due to ocean tidal flow, CHAMP Mission Results II, Springer Berlin, 359– 65.

Lühr H., M. Rother, S. Maus, W. Mai, D. Cooke; The diamagnetic effect of the equatorial Appleton anomaly: Its characteristics and impact on geomagnetic field modeling, Geophys. Res. Lett., 30 (17), 1906, doi:10.1029/2003GL017407, 2003.

Maus, S., and Silva, L., and Hulot, G., Can core-surface flow models be used to improve the forecast of the Earth's main magnetic field? Journal of Geophysical Research, 113, B08102, doi:10.1029/2007JB005199, 2008

Maus, S. & Lühr, H., Signature of the quiet-time magnetospheric magnetic field and its electromagnetic induction in the rotating Earth,Geophys. J. Int., 162, 755-763, doi: 10.1111/j.1365-246X.2005.02691.x, 2005

Olsen, N., Hermann Luehr, Terence J. Sabaka, Mioara Mandea, Martin Rother, Lars Tøffner-Clausen, Sungchan Choi, CHAOS - A Model of Earth's Magnetic Field derived from CHAMP, Ørsted, and SAC-C magnetic satellite data, Geoph. J. Int., 166, 67-75, doi: 10.1111/j.1365-246X.2006.02959.x, 2006)